Modeling how early passive immunization with broadly neutralizing antibodies elicits lasting control of SHIV infection

Authors: Rajat Desikan[1†], Rubesh Raja[1†], Narendra. M. Dixit[1,2*]

Affiliations:

[1]Department of Chemical Engineering, Indian Institute of Science, Bengaluru, India, 560012.

[2]Centre for Biosystems Science and Engineering, Indian Institute of Science, Bengaluru, India, 560012.

*To whom correspondence should be addressed: narendra@iisc.ac.in

†These authors contributed equally to this work.

One Sentence Summary: Mathematical modelling elucidates the pleiotropic effects of HIV-1 broadly neutralizing antibodies that underlie lasting viremic control following early passive immunization and suggests strategies for achieving functional cure of HIV-1 infection.

Abstract: Passive immunization with broadly neutralizing antibodies (bNAbs) of HIV-1 early in infection was shown recently to elicit long-term viremic control in a majority of SHIV-infected macaques treated, raising hopes of a functional cure of HIV-1 infection. Here, we developed a mathematical model of viral dynamics with bNAb therapy, analyzed *in vivo* data, and elucidated the mechanisms underlying the observed lasting control. We found that pleiotropic effects of bNAbs were responsible for lasting control: bNAbs enhanced antigen uptake, stimulating cytotoxic T lymphocytes (CTLs), and suppressed viremia, limiting CTL exhaustion. When the administered bNAbs were cleared from circulation, viremia rose but in the presence of a primed CTL population, which eventually controlled the infection. Our model fit the complex patterns of viral load changes observed quantitatively. Model predictions identify optimal bNAb-based interventions and suggest that bNAbs combined with antiretroviral therapy may elicit functional cure also of chronic HIV-1 infection.

Document statistics:

Title = 118 characters including spaces | Words in abstract = 147 | Words in main text and references (excluding figure captions) = ~5000 | Figures = 3 | References = 49 | Supplementary methods = yes | Supplementary figures = 7 | Supplementary tables = 6 | Supplementary references = 22

Introduction

Current antiretroviral therapies (ART) for HIV-1 infection control viremia in infected individuals but are unable to eradicate the virus (*1*). A reservoir of latently infected cells, which is established soon after infection (*2*), escapes drugs and the host immune response (*3*), is long-lived (*4, 5*), and can reignite infection following the cessation of therapy (*6*), presents the key obstacle to sterilizing cure. Efforts are now aimed at eliciting a "functional cure" of the infection, where the virus can be controlled without life-long treatment even though eradication is not possible (*7, 8*). That functional cure can be achieved has been demonstrated by the VISCONTI trial, where a subset of patients, following early initiation of ART, maintained undetectable viremia long after the cessation of treatment (*9*). A limitation, however, is that the subset that achieves post-treatment control with ART is small, 5-15% of the patients treated (*10*). In a spectacular study last year, Nishimura *et al.* (*11*) found that early, short-term passive immunization with a combination of two HIV-1 broadly neutralizing antibodies (bNAbs) elicited lasting control of viremia in 10 of 13, or nearly 77%, of SHIV-infected macaques treated. This high success rate raises the prospect of achieving functional cure in all HIV-1 infected individuals using short-term bNAb therapy.

Devising passive immunization protocols that would maximize the chances of achieving functional cure requires an understanding of the mechanism(s) with which early, short-term passive immunization with bNAbs induces sustained control of viremia. Nishimura *et al.* (*11*) argue that the control they observed, lasting long (years) after the administered bNAbs were cleared from circulation (weeks), was due to the effector function of cytotoxic $CD8^+$ T lymphocytes (CTLs) because transient suppression of CTLs, using anti-CD8 antibodies (Abs), well after the establishment of control resulted in a temporary surge of viremia. How short-term bNAb therapy leads to sustained CTL stimulation, and therefore lasting viremic control, remains unknown.

Here, we constructed a mathematical model of viral dynamics in the presence of bNAbs, using which we quantitatively analyzed longitudinal *in vivo* viral load data and elucidated the mechanisms underlying the lasting viremic control elicited by early, short-term bNAb therapy. Using the model, we asked whether bNAb therapy can be rationally optimized and employed to achieve functional cure also of chronic HIV-1 infection.

Results

Mathematical model of viral dynamics with passive immunization

We constructed a mathematical model that considered the within-host dynamics of populations of target $CD4^+$ T cells, productively and latently infected cells, free virions, antigen presenting cells (APCs), effector CTLs, and administered bNAbs (Figure 1). Based on the known effects of bNAbs (*12-16*), we let bNAbs 1) enhance the clearance of free virions and 2) increase antigen uptake by APCs, both in a dose-dependent manner. CTLs were stimulated by APCs and could become exhausted by sustained antigenic stimulation. By lowering antigen levels, bNAbs could reverse CTL exhaustion. ART was assumed to reduce the productive infection of target cells. Anti-CD8 Abs were assumed to reduce the CTL population and compromise host effector functions for a duration corresponding to the residence time of the depleting Abs in circulation.

We constructed equations to describe the resulting dynamics and solved them using parameter values representative of SHIV infection of macaques (Methods).

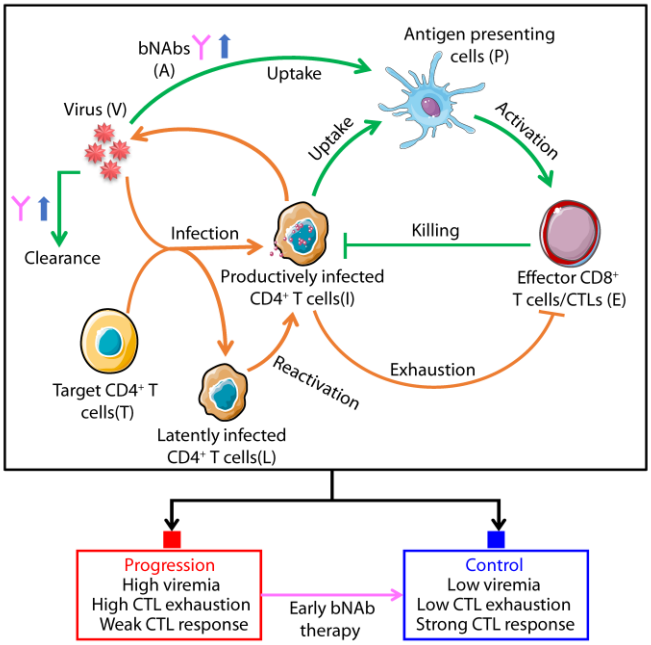

Figure 1: Schematic of the mathematical model of SHIV dynamics with bNAb therapy. Orange and green arrows indicate processes involved in the growth and control of infection, respectively. The steps influenced by bNAbs are shown with thick blue arrows. Corresponding model equations are described in Methods. Steady state analysis of the model indicates two fates of the infection: chronic infection with high viremia that marks progressive disease (red filled square), typically realized in the absence of treatment, and viremic control (blue filled square), orchestrated by early bNAb therapy.

Model predictions fit in vivo data

We applied the model to describe the viral load changes reported in Nishimura *et al.* (*11*) where 3 weekly infusions of a combination of two HIV-1 bNAbs, 3BNC117 and 10-1074, starting from day 3 post SHIV challenge were administered. We considered the 10 "responder" macaques who showed no significant decline in $CD4^+$ T cell counts and included 6 with undetectable post-treatment set-point viremia ($<10^2$ copies/mL), termed controllers, and 4 with detectable but low post-treatment set-point viremia ($<10^3$ copies/mL). To determine bNAb levels in circulation, we mimicked the dosing protocol employed in the experiments (Methods) and estimated the bNAb half-lives from exponential fits to measured bNAb levels in each macaque (Figure S1 and Table S1). Where available, we fixed model parameter values from previous studies (Table S2). We then fit model predictions to data, letting the remaining parameters be adjustable, following a two-step procedure: We first fit the averaged viral load data in the acute infection phase in treated and untreated macaques simultaneously (Methods, Figure S2 and Table S3). Next, we fit the long-term viral load data of the individual controller macaques (Figure 2,

Figure S3, Table S4, Table S5). The two-step procedure, using suitable objective functions that we constructed (Table S6), enabled robust parameter estimation and fitting the complex temporal dynamics observed. Constrained optimization with penalty functions has been used recently to fit data following CD8+ T cell depletion in macaques to assess the role of CTLs in viremic control (*17*).

We considered first the macaque DEWL for which the most data was available (Figure 2A). The viral dynamics during and post bNAb therapy could be divided into the following phases. Viremia dropped post the acute infection peak to undetectable levels (<10^2 copies/mL), where it remained until the administered bNAbs were cleared from circulation (Phase I in Figure 2A). Shortly thereafter, viremia resurged to an elevated level (~10^5 copies/mL), well above the acute infection peak (<10^4 copies/mL), but subsequently declined spontaneously to a low (10^2-10^3 copies/mL) level (Phase II), where it remained for the rest of the duration of follow-up (>3 years; Phase III). Following the administration of anti-CD8 Abs, several months after the establishment of control, viremia immediately resurged to high levels again, but was eventually controlled (Phase IV). Remarkably, our model provided an excellent fit to the entire time-course (Figure 2A).

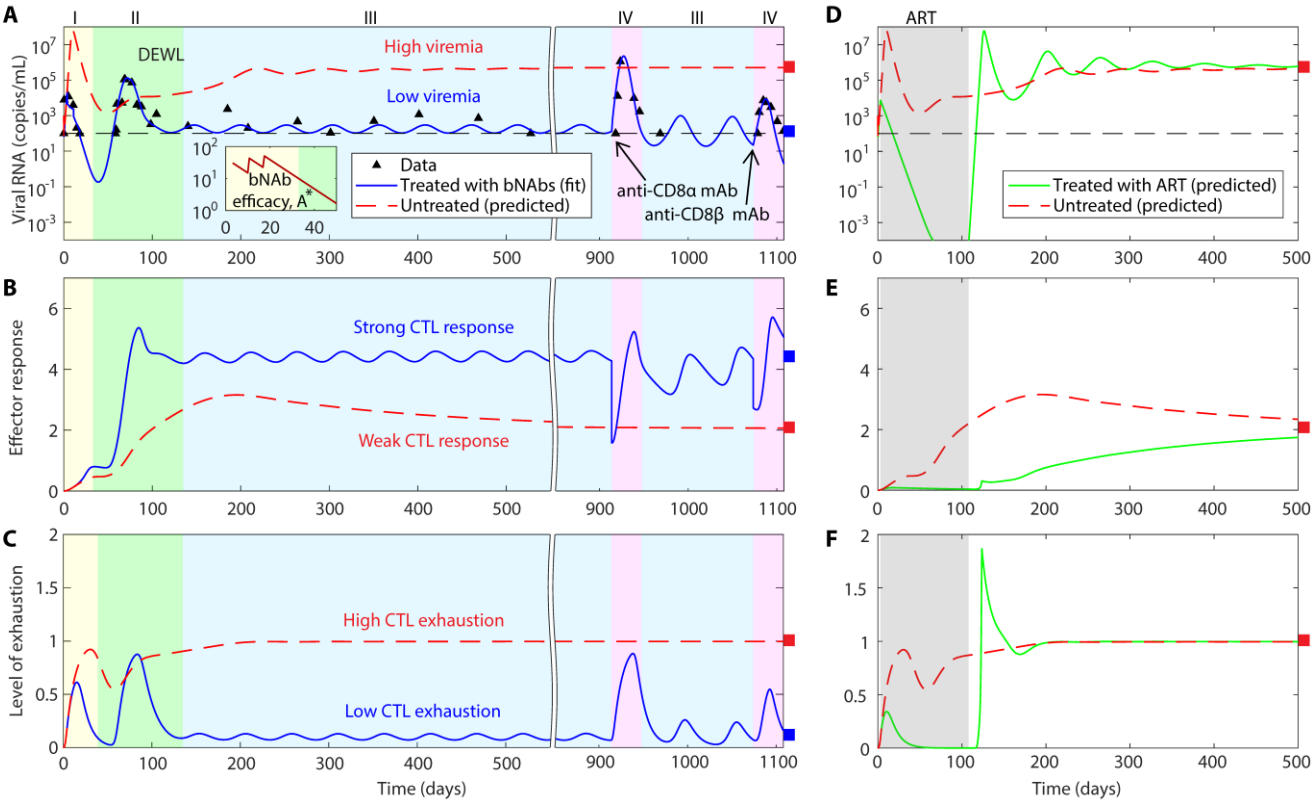

Figure 2: Mathematical model quantitatively describes viral load data and elucidates mechanisms of bNAb-induced viremic control. (A) Model fit (blue line) to viral load data (*11*) (symbols) in the responder macaque DEWL. (Fits for the other responder macaques are in Figure S3.) The corresponding dynamics of the bNAb concentrations (inset in A), CTL response (B), and the level of CTL exhaustion (C) are shown. Phase I (yellow) marks the duration when bNAbs are present in circulation, phase II (green) the viremic resurgence post the clearance of bNAbs, phase III (blue) the ensuing viremic control, and phase IV (pink), in two parts, the disruption of this

control using anti-CD8α and anti-CD8β Abs, respectively. Red dashed lines in all panels indicate predictions in the absence of bNAb therapy. ART fails to establish long-term viremic control in macaques, as shown by the simulated dynamics of viral load (D), CTL response (E) and CTL exhaustion (F) with ART (green lines). The duration of ART is shown as a grey region. Black dashed lines in (A) and (D) indicate the viral load detection limit (100 RNA copies/mL).

We repeated the fitting with the other 9 responder macaques. The viral dynamics was similarly complex in these macaques, but less data was available than for DEWL. We obtained excellent fits to data from 7 of the 9 responder macaques (Figure S3). Two macaques (DFIK and DEWP) had no or limited detectable viremia, which precluded fitting (Figure S3). One macaque (DFIK) lost control following the administration of anti-CD8 Abs and reached a high viral load set-point, akin to untreated macaques. Our model reproduced the latter observation when the extent of CTL depletion due to the anti-CD8 Abs was increased (Figure S3 top panel).

The ability to describe the complex viral load changes during and post bNAb therapy quantitatively gave us confidence in our model. We applied our model next to elucidate the mechanistic origins of the observed long-term viremic control.

Pleiotropic effects of bNAbs underlie lasting viremic control

We hypothesized, following previous analyses of post-treatment control with ART (*18*), that the lasting control observed with early bNAb therapy was a distinct steady state of the system. Indeed, solving our model equations (Methods), we identified two underlying stable steady states, which we indicate with red and blue filled squares, respectively, in all the figures. The first had high viremia, high levels of CTL exhaustion and weak CTL effector function, marking chronic infection leading to progressive disease. The second had low viremia, low levels of CTL exhaustion and strong CTL effector function, indicating lasting control. These states existed over wide ranges of parameter values (Figure S4).

When a new infection occurs, viremia rises significantly during the acute infection phase and achieves high levels typically before a CTL response is mounted (*19*). The CTL response thus lags and is dominated by the virus. If left untreated, the high viremic fate, leading to progressive disease, is realized. This behaviour is consistent with observations of untreated macaques challenged with SHIV (*20, 21*), which our model recapitulates (red lines in Figure 2A-C). Following the initial transients, a high viremia, a high level of exhaustion, and a weak CTL response result.

Early bNAb therapy drove the infection to the fate of lasting viremic control (blue lines in Figure 2A-C), in agreement with the observations in Nishimura *et al.* (*11*). Pleiotropic effects of bNAbs were involved in orchestrating this transition. During acute infection, bNAbs suppressed the viremic peak by enhancing viral clearance. The lower viremia limited CTL exhaustion. Further, bNAbs increased antigen presentation and CTL stimulation. When the administered bNAbs were cleared, viremia resurged but in the presence of a primed CTL population, which was larger and less severely exhausted than in untreated macaques (Figure 2A, B). The primed CTL population was able to control the infection.

We may construe the rise in viremia post the clearance of the administered bNAbs as arising from a new infection but under conditions where the CTL population is primed and thus

has a head start over the virus. Indeed, our model calculations of the hypothetical scenario where a higher CTL population existed at the time of viral challenge showed spontaneous control (Figure S5). Similarly, suppression of CTLs up to a threshold after the establishment of control allowed resurgence in viremia but restored control, whereas suppression beyond the threshold sacrificed control and drove infection to the former, high viremic fate (Figure S3 top), explaining the difference between the controller macaques who reasserted viremic control following the transient rise in viremia upon the administration of anti-CD8 Abs and the one controller macaque that failed to reassert control and transitioned to the high viremic state (*11*). When we repeated our analysis without either enhanced clearance of virus or upregulation of antigen presentation by bNAbs, our model failed to capture the observed viral load data robustly (Figure S6). Specifically, when we fit our model without bNAb-induced upregulation of antigen presentation, the resulting best-fit parameters were such that a 1 $\log_{10}$ lower viral inoculum resulted in the loss of viral control, which cannot be justified, whereas a model without enhanced viral clearance failed to fit the data (Figure S6). The rapid clearance of the virus, which lowered viremia and reversed CTL exhaustion, together with increased Ag uptake, which led to enhanced CTL stimulation, thus resulted in the lasting control of viremia elicited by early, short-term bNAb therapy.

bNAbs have an advantage over ART

If ART were used instead of bNAbs, for a duration equivalent to the time over which administered bNAbs were in circulation, viral load quickly became undetectable during treatment but rebound to high levels post treatment (Figure 2D-F), consistent with the 3 macaques administered ART in Nishimura *et al.* (*11*). While both bNAb therapy and ART limited viremia (Figure 2A, D) and thus prevented CTL exhaustion (Figure 2C, F), bNAb therapy additionally increased antigen presentation and CTL stimulation (Figure 2B, E). The resurgence in viremia post the cessation of ART was thus akin to *de novo* infection, which typically reaches the high viremic fate. Only in the rare individuals in whom the latent reservoir is sufficiently small is this rise in viremia small enough for the CTL population to catch up and establish control, explaining the critical role of the size of the latent reservoir in post treatment control with ART (*18*). The primed CTL population following bNAb therapy, in contrast, drove the system to viremic control. The pleiotropic effects of bNAbs thus confer a significant advantage upon bNAbs over ART, explaining the much higher success rate of bNAbs in achieving functional cure.

Strategies to maximize the impact of bNAb therapy

One possibility underlying the failure of bNAb therapy in 3 macaques in Nishimura *et al.* (*11*) could be inadequate bNAb efficacy. Maximum bNAb concentrations and bNAb half-lives varied substantially across macaques (*11*). We therefore performed calculations over a wide range of maximum bNAb concentrations and bNAb half-lives and examined the long-term fate that would be realized given the dosing protocol in Nishimura *et al.* (*11*). We found that for any bNAb half-life, a threshold level of the maximum bNAb concentration existed above which viremic control was established and below which the high viremic, progressive state resulted (Figure 3A). The threshold decreased as the half-life increased. The bNAb half-life and the maximum bNAb concentration could be measured in an infected individual. If the combination

were to lie in the region where control is not expected, a higher dosage and/or an enhanced half-life could ensure control (Figure 3B). Sustained bNAb activity could be achieved with additional dosages or with other bNAbs and engineered variants that have intrinsically longer half-lives (*22*, *23*).

bNAbs could also be administered during chronic infection (*21*, *24*). The high viremia together with the high genomic diversity present in the chronic phase (*25*) may result in the rapid development of resistance to bNAbs (*26*, *27*). The genetic barrier bNAb combinations must offer to avert resistance remains to be established. Alternatively, ART could be employed to control viremia, given that ART combinations have been optimized to prevent resistance (*28*), and then a short bNAb course could elicit functional cure. Our model predicts that such a strategy is likely to succeed. We let ART be administered for 15 weeks during chronic infection by the end of which viremia was well below detection. ART was then stopped and 3 days later a course of 3 weekly bNAb doses was administered. Whereas viremia resurged to high levels without the latter course, the bNAb course successfully established viremic control (Figure 3C-E).

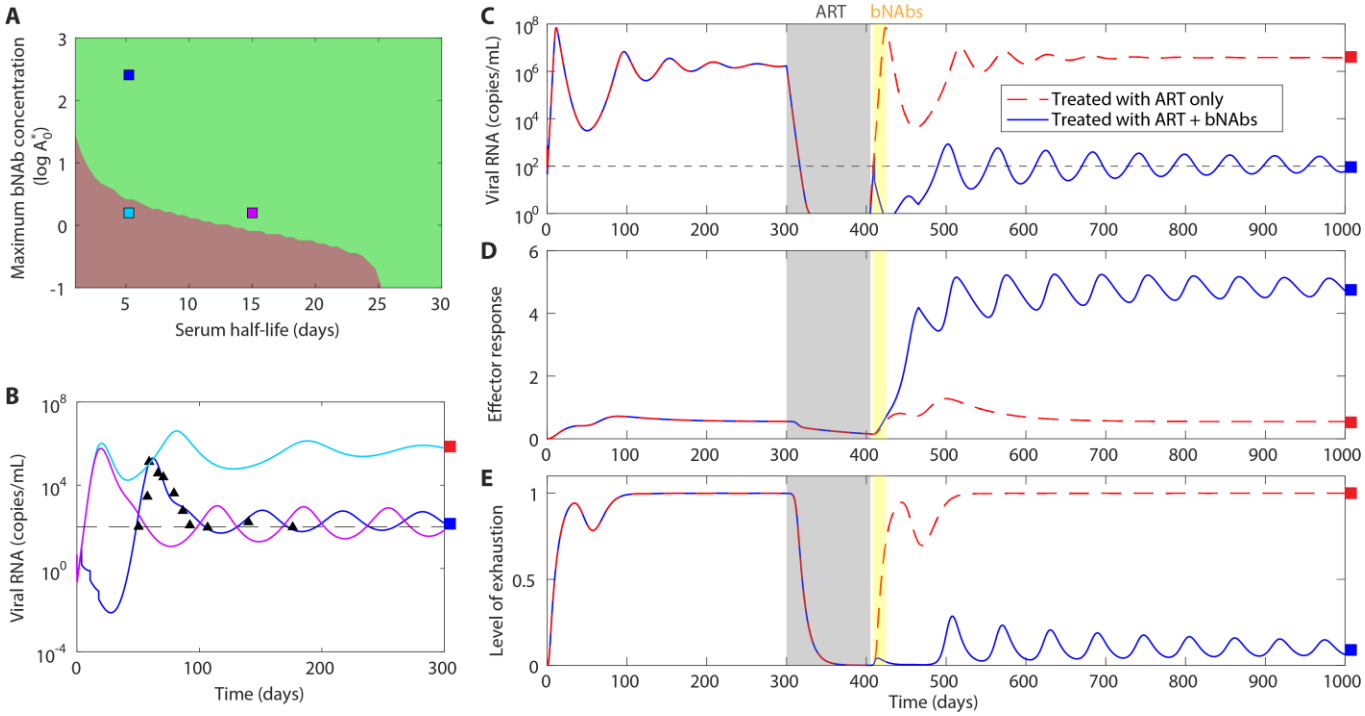

Figure 3: Strategies to optimize bNAb therapy. (A) Phase boundary on the maximum bNAb concentration *versus* bNAb half-life plot separating conditions yielding viremic control (green) from those leading to progressive disease (brown). (B) Representative viral dynamics showing treatment failure (cyan) that can be averted with a higher bNAb dose (blue) or half-life (magenta). The corresponding conditions in the phase diagram in (A) are indicated with similarly colored boxes. The blue box and line mimic conditions of the macaque MVJ in Figure S3 and the corresponding data is reproduced in (B) for comparison. (C-E) Passive bNAb immunization following ART during chronic infection can elicit functional cure. Dynamics of viral load (C), CTL response (D) and CTL exhaustion (E) predicted by the model are shown for intervention with ART (gray region) either followed by (blue lines) 3 weekly bNAb infusions starting 3 days after the cessation of ART (yellow region) or not (red lines). Black dashed lines in (B) and (C) indicate the viral load detection limit (100 RNA copies/mL).

Discussion

The recent success of passive immunization with bNAbs in eliciting functional cure of HIV-1 infection can potentially revolutionize HIV-1 care (*11, 15, 29-32*). In this study, using mathematical modelling and analysis of *in vivo* data, we elucidated the pleiotropic effects of bNAbs responsible for inducing lasting viremic control following a short, early passive immunization course, and suggest strategies to use bNAbs for achieving functional cure in acute as well as chronic HIV-1 infection.

Our study makes significant advances over previous studies on understanding functional cure as well as the influence of bNAbs. Post-treatment control following ART has been explained using a mathematical model as one of two underlying stable steady states (*18*), which is consistent with our findings. Here, we capture not only the steady states, but, for the first time, also the complex dynamics of longitudinal viral load changes, presenting a more comprehensive understanding of functional cure. The ability to describe dynamics allows us to predict threshold bNAb half-lives/concentrations that would ensure functional cure, potentially improving outcomes of bNAb therapies and informing Ab engineering strategies (*23*).

A mathematical model was employed recently to analyse short-term viral load changes following passive immunization with bNAbs, based on which bNAbs were argued not only to enhance the clearance of free virions but also the loss of infected cells (*14*). The link to lasting control remained to be established. Here, we found that enhanced viral clearance and antigen presentation, which not only suppressed viremia, but also enhanced CTL stimulation and prevented CTL exhaustion, collectively induced functional cure. The difference between ART and bNAb therapy in inducing functional cure thus became evident. ART suppressed viremia but did not enhance antigen presentation, explaining its lower success rates compared to bNAb therapy in inducing functional cure. From a dynamical systems perspective, following *de novo* infection, viral levels rise before a strong CTL response can be mounted, leading typically to CTL exhaustion and progressive disease with high viremia. bNAbs tilt the competition in favour of CTLs and induce lasting viral control.

It follows that other strategies that similarly tilt the balance in favour of CTLs may also lead to functional cure. For instance, ART can reverse CTL exhaustion by suppressing viremia. Our model suggests that a short course of bNAbs following ART may induce functional cure also of chronic HIV-1 infection. Similarly, immune checkpoint inhibitors can prevent CTL exhaustion during infection (*33*). CTLs can also be stimulated using vaccines (*34*). Our model predicts that a primed CTL population at the time of viral challenge may prevent the infection from reaching the high viremic, progressive state and drive it instead to lasting viremic control, indicating a potentially favourable outcome of prophylactic T cell vaccines. Stimulating CTLs using vaccines has been shown to suppress viral replication and lower the set-point viremia (*35, 36*), but several additional design challenges must be overcome, including the need to stimulate CTLs early enough and, interestingly, prevent CTL exhaustion due to the vaccine (*37*), for the successful deployment of T cell vaccines (*38*). Future studies may test whether these latter strategies, independently or in combination with bNAbs, can improve the chances of achieving functional cure.

In two significant studies this year, the same bNAb combination therapy used by Nishimura et al. (*11*) was extended to humans who were either untreated or on treatment interruption following viral suppression with ART (*29, 30*). The bNAb therapy was well

tolerated and suppressed viremia akin to macaques. When viremia rose following the clearance of the administered bNAbs, the patients were (re)started on ART, precluding the possible establishment of spontaneous long-term control observed in the responder macaques in Nishimura et al. (*11*).

Following the observation of Nishimura *et al.* (*11*) that there was no significant generation of anti-gp120 Abs in controllers, we ignored the ability of bNAbs to upregulate the humoral response (*39*). Our study is thus conservative in its assessment of the influence of bNAbs. We did not consider data where functional cure is not established and $CD4^+$ T cell counts gradually decline. Models invoking pyroptosis (*40*) may be required to describe the gradual $CD4^+$ T cell decline leading to AIDS (*41*). The essential idea, however, of the two distinct fates of infection and the ability of bNAbs to induce a switch between them is expected to hold because pyroptosis determines how $CD4^+$ T cell counts decline *after* the establishment of the high viremic state and, also, it is expected not be a significant force when viremia is controlled. Finally, we did not consider viral evolution and resistance to bNAbs, recognizing that the controllers in Nishimura *et al.* (*11*) saw no resistance. Future studies on larger populations and with other combinations of bNAbs may determine whether resistance must be accounted for in defining optimal treatments.

In summary, our study presents the first quantitative description of viral dynamics following passive immunization with HIV-1 bNAbs; captures *in vivo* data; elucidates the mechanisms with which early, short-term bNAb therapy establishes lasting viremic control of SHIV infection; and presents avenues to maximize the success rate of bNAb therapies in inducing functional cure of HIV-1 infection.

Materials and Methods

Mathematical model

We constructed the following equations to describe the viral dynamics depicted schematically in Figure 1.

$$\frac{dT}{dt} = \lambda_T - d_T T - \beta V T \tag{1}$$

$$\frac{dL}{dt} = f_L \beta V T + \left(\psi - a - d_L\right) L \tag{2}$$

$$\frac{dI}{dt} = \left(1 - f_L\right) \beta V T + aL - \left(d_I + mE\right) I \tag{3}$$

$$\frac{dV}{dt} = pI - cV - k_A A V \tag{4}$$

$$\frac{dP}{dt} = \gamma I + f k_A A V - d_P P \tag{5}$$

$$\frac{dE}{dt} = \frac{\left(\rho + k_E E\right) P}{\phi_1 + P} - \left(\frac{\xi Q^n}{q_c^n + Q^n} + d_E\right) E \tag{6}$$

$$\frac{dQ}{dt} = \kappa\left(\frac{I}{\phi_2 + I}\right) - d_q Q \tag{7}$$

$$A = A_0 \sum_{i=1}^{3} e^{-\eta\left(t-\left(\tau_i+\omega\right)\right)} H(t-\left(\tau_i+\omega\right)) \tag{8}$$

Here, target CD4$^+$ T cells, *T*, are produced at the rate λ_T, die at the per capita rate d_T, and are infected by virions, *V*, with the second order rate constant β. A fraction f_L of these infections yields latently-infected cells (*18*), *L*, and the rest, productively-infected cells, *I*. Cells *L* proliferate, get activated, and die at the per capita rates ψ, *a*, and d_L, respectively. Cells *I* die at the per capita rate d_I due to viral cytopathicity and are killed by effector CTLs, *E*, with the second order rate constant *m*. Cells *I* produce free virions at the rate *p* per cell. The virions are cleared (*12, 42, 43*) in the absence of administered bNAbs with the rate constant *c*. Administered bNAbs enhance the viral clearance rate by a time-dependent amount, $k_A AV$, proportional to the instantaneous serum concentration of the bNAbs, *A*, with the proportionality constant k_A. APCs are assumed not to be limiting and take up SHIV-specific antigen from *I* for presentation with the first-order rate constant γ. Administered bNAbs increase antigen uptake with the rate $fk_A AV$, where *f* depicts the effect of the bNAbs on antigen uptake relative to viral clearance. SHIV-specific APCs, *P*, are lost at the per capita rate d_p. They stimulate naïve CD8$^+$ T cells (*44, 45*), assumed not to be limiting, into SHIV-specific CTLs, *E*, with the maximal rate ρ and the half-maximal parameter ϕ_1. CTLs proliferate (*46*) with the rate constant k_E, and suffer exhaustion (*45, 47*) at the maximal rate ξ, with the half-maximal parameter q_c and Hill coefficient *n*. The level of exhaustion, *Q*, increases with antigen level at the maximal rate κ and with the half-maximal parameter ϕ_2. Exhaustion is reversed with the rate constant d_q. CTLs are lost (*48, 49*) at the per capita rate d_E. Alternative descriptions of CTL stimulation and exhaustion have been proposed but do not alter the key model predictions (*18, 45*) (Text S1 and Figure S7).

To mimic the dosing protocol in Nishimura *et al.* (*11*), we let *A* rise by the extent A_0 immediately upon the administration of a bNAb dose, and decline exponentially with the rate constant η. The three doses were administered on days $\tau_1 = 3$, $\tau_2 = 10$, and $\tau_3 = 17$, respectively. Additionally, we allowed a delay in bNAb action, ω, following each dose, to account for any pharmacological effects within individual macaques. The Heaviside function, $H\left(t < \left(\tau_i + \omega\right)\right) = 0$ and $H\left(t > \left(\tau_i + \omega\right)\right) = 1$, accounts for bNAb dynamics based on these dosing times. To compare the influence of bNAbs with that of ART, we assumed that ART reduces β by a factor $1-\epsilon$, where ϵ is the efficacy of the drug combination (*18*).

Long after bNAbs were cleared from circulation, Nishimura *et al.* (*11*) administered anti-CD8α antibodies to some macaques, which resulted in the depletion of CD8$^+$ T, NK, NKT, and $\gamma\delta$ T cells. Nishimura *et al.* (*11*) also administered anti-CD8β antibodies to some macaques, which only depleted CD8$^+$ T cells. To describe the resulting changes in viremia, we assumed that the depleting effects of anti-CD8α and anti-CD8β antibodies started at time points θ_α and θ_β, respectively, at which points we reduced the CTL populations by fractions ζ_α and ζ_β. Further,

we assumed that anti-CD8α antibodies neutralized all host effector functions, which we modelled by setting $m = 0$ for a duration θ_m representing the residence time of the depleting antibodies.

The procedures for solving the above model equations, parameter estimation, and data fitting have been described in the supplementary methods. All the data employed for fitting was obtained by digitizing the data published in Nishimura et al. (*11*) using the software Engauge digitizer.

Acknowledgements
We thank Alan Perelson and Rustom Antia for comments on an earlier version of our manuscript.

Funding
This work was supported by the Wellcome Trust/DBT India Alliance Senior Fellowship IA/S/14/1/501307 (NMD).

Author Contributions
R.D., R.R. and N.M.D. conceptualized and designed the study. R.D. and R.R. simulated the model, fit predictions to data and estimated parameters. R.D., R.R. and N.M.D. analyzed results and wrote the manuscript.

References

1. N. M. Archin, J. M. Sung, C. Garrido, N. Soriano-Sarabia, D. M. Margolis, Eradicating HIV-1 infection: seeking to clear a persistent pathogen. *Nat. Rev. Microbiol.* **12**, 750-764 (2014).
2. J. B. Whitney, A. L. Hill, S. Sanisetty, P. Penaloza-MacMaster, J. Liu, M. Shetty, L. Parenteau, C. Cabral, J. Shields, S. Blackmore, J. Y. Smith, A. L. Brinkman, L. E. Peter, S. I. Mathew, K. M. Smith, E. N. Borducchi, D. I. Rosenbloom, M. G. Lewis, J. Hattersley, B. Li, J. Hesselgesser, R. Geleziunas, M. L. Robb, J. H. Kim, N. L. Michael, D. H. Barouch, Rapid seeding of the viral reservoir prior to SIV viraemia in rhesus monkeys. *Nature* **512**, 74-77 (2014).
3. Y. C. Ho, L. Shan, N. N. Hosmane, J. Wang, S. B. Laskey, D. I. Rosenbloom, J. Lai, J. N. Blankson, J. D. Siliciano, R. F. Siliciano, Replication-competent noninduced proviruses in the latent reservoir increase barrier to HIV-1 cure. *Cell* **155**, 540-551 (2013).
4. D. Finzi, J. Blankson, J. D. Siliciano, J. B. Margolick, K. Chadwick, T. Pierson, K. Smith, J. Lisziewicz, F. Lori, C. Flexner, T. C. Quinn, R. E. Chaisson, E. Rosenberg, B. Walker, S. Gange, J. Gallant, R. F. Siliciano, Latent infection of CD4+ T cells provides a mechanism for lifelong persistence of HIV-1, even in patients on effective combination therapy. *Nat. Med.* **5**, 512-517 (1999).

5. J. D. Siliciano, J. Kajdas, D. Finzi, T. C. Quinn, K. Chadwick, J. B. Margolick, C. Kovacs, S. J. Gange, R. F. Siliciano, Long-term follow-up studies confirm the stability of the latent reservoir for HIV-1 in resting CD4+ T cells. *Nat. Med.* **9**, 727-728 (2003).
6. B. Joos, M. Fischer, H. Kuster, S. K. Pillai, J. K. Wong, J. Boni, B. Hirschel, R. Weber, A. Trkola, H. F. Gunthard, H. I. V. C. S. Swiss, HIV rebounds from latently infected cells, rather than from continuing low-level replication. *Proc. Natl. Acad. Sci. U. S. A.* **105**, 16725-16730 (2008).
7. A. S. S. W. G. o. H. I. V. C. International, S. G. Deeks, B. Autran, B. Berkhout, M. Benkirane, S. Cairns, N. Chomont, T. W. Chun, M. Churchill, M. Di Mascio, C. Katlama, A. Lafeuillade, A. Landay, M. Lederman, S. R. Lewin, F. Maldarelli, D. Margolis, M. Markowitz, J. Martinez-Picado, J. I. Mullins, J. Mellors, S. Moreno, U. O'Doherty, S. Palmer, M. C. Penicaud, M. Peterlin, G. Poli, J. P. Routy, C. Rouzioux, G. Silvestri, M. Stevenson, A. Telenti, C. Van Lint, E. Verdin, A. Woolfrey, J. Zaia, F. Barre-Sinoussi, Towards an HIV cure: a global scientific strategy. *Nat. Rev. Immunol.* **12**, 607-614 (2012).
8. M. Perreau, R. Banga, G. Pantaleo, Targeted immune interventions for an HIV-1 cure. *Trends Mol. Med.* **23**, 945-961 (2017).
9. A. Saez-Cirion, C. Bacchus, L. Hocqueloux, V. Avettand-Fenoel, I. Girault, C. Lecuroux, V. Potard, P. Versmisse, A. Melard, T. Prazuck, B. Descours, J. Guergnon, J. P. Viard, F. Boufassa, O. Lambotte, C. Goujard, L. Meyer, D. Costagliola, A. Venet, G. Pancino, B. Autran, C. Rouzioux, A. V. S. Group, Post-treatment HIV-1 controllers with a long-term virological remission after the interruption of early initiated antiretroviral therapy ANRS VISCONTI Study. *PLoS Pathog.* **9**, e1003211 (2013).
10. L. R. Cockerham, H. Hatano, S. G. Deeks, Post-treatment controllers: role in HIV "cure" research. *Curr. HIV/AIDS Rep.* **13**, 1-9 (2016).
11. Y. Nishimura, R. Gautam, T. W. Chun, R. Sadjadpour, K. E. Foulds, M. Shingai, F. Klein, A. Gazumyan, J. Golijanin, M. Donaldson, O. K. Donau, R. J. Plishka, A. Buckler-White, M. S. Seaman, J. D. Lifson, R. A. Koup, A. S. Fauci, M. C. Nussenzweig, M. A. Martin, Early antibody therapy can induce long-lasting immunity to SHIV. *Nature* **543**, 559-563 (2017).
12. T. Igarashi, C. Brown, A. Azadegan, N. Haigwood, D. Dimitrov, M. A. Martin, R. Shibata, Human immunodeficiency virus type 1 neutralizing antibodies accelerate clearance of cell-free virions from blood plasma. *Nat. Med.* **5**, 211-216 (1999).
13. J. Liu, K. Ghneim, D. Sok, W. J. Bosche, Y. Li, E. Chipriano, B. Berkemeier, K. Oswald, E. Borducchi, C. Cabral, L. Peter, A. Brinkman, M. Shetty, J. Jimenez, J. Mondesir, B. Lee, P. Giglio, A. Chandrashekar, P. Abbink, A. Colantonio, C. Gittens, C. Baker, W. Wagner, M. G. Lewis, W. Li, R. P. Sekaly, J. D. Lifson, D. R. Burton, D. H. Barouch, Antibody-mediated protection against SHIV challenge includes systemic clearance of distal virus. *Science* **353**, 1045-1049 (2016).
14. C. L. Lu, D. K. Murakowski, S. Bournazos, T. Schoofs, D. Sarkar, A. Halper-Stromberg, J. A. Horwitz, L. Nogueira, J. Golijanin, A. Gazumyan, J. V. Ravetch, M. Caskey, A. K. Chakraborty, M. C. Nussenzweig, Enhanced clearance of HIV-1-infected cells by broadly neutralizing antibodies against HIV-1 *in vivo*. *Science* **352**, 1001-1004 (2016).
15. Y. Nishimura, M. A. Martin, Of mice, macaques, and men: broadly neutralizing antibody immunotherapy for HIV-1. *Cell Host Microbe* **22**, 207-216 (2017).

16. L. L. Lu, T. J. Suscovich, S. M. Fortune, G. Alter, Beyond binding: antibody effector functions in infectious diseases. *Nat. Rev. Immunol.* **18**, 46-61 (2018).
17. Y. Cao, E. K. Cartwright, G. Silvestri, A. S. Perelson, CD8+ lymphocyte control of SIV infection during antiretroviral therapy. *PLoS Pathog.* **14**, e1007350 (2018).
18. J. M. Conway, A. S. Perelson, Post-treatment control of HIV infection. *Proc. Natl. Acad. Sci. U. S. A.* **112**, 5467-5472 (2015).
19. N. Goonetilleke, M. K. Liu, J. F. Salazar-Gonzalez, G. Ferrari, E. Giorgi, V. V. Ganusov, B. F. Keele, G. H. Learn, E. L. Turnbull, M. G. Salazar, K. J. Weinhold, S. Moore, C. C. C. B, N. Letvin, B. F. Haynes, M. S. Cohen, P. Hraber, T. Bhattacharya, P. Borrow, A. S. Perelson, B. H. Hahn, G. M. Shaw, B. T. Korber, A. J. McMichael, The first T cell response to transmitted/founder virus contributes to the control of acute viremia in HIV-1 infection. *J. Exp. Med.* **206**, 1253-1272 (2009).
20. R. Gautam, Y. Nishimura, W. R. Lee, O. Donau, A. Buckler-White, M. Shingai, R. Sadjadpour, S. D. Schmidt, C. C. LaBranche, B. F. Keele, D. Montefiori, J. R. Mascola, M. A. Martin, Pathogenicity and mucosal transmissibility of the R5-tropic simian/human immunodeficiency virus SHIV(AD8) in rhesus macaques: implications for use in vaccine studies. *J. Virol.* **86**, 8516-8526 (2012).
21. M. Shingai, Y. Nishimura, F. Klein, H. Mouquet, O. K. Donau, R. Plishka, A. Buckler-White, M. Seaman, M. Piatak, Jr., J. D. Lifson, D. S. Dimitrov, M. C. Nussenzweig, M. A. Martin, Antibody-mediated immunotherapy of macaques chronically infected with SHIV suppresses viraemia. *Nature* **503**, 277-280 (2013).
22. S. Y. Ko, A. Pegu, R. S. Rudicell, Z. Y. Yang, M. G. Joyce, X. Chen, K. Wang, S. Bao, T. D. Kraemer, T. Rath, M. Zeng, S. D. Schmidt, J. P. Todd, S. R. Penzak, K. O. Saunders, M. C. Nason, A. T. Haase, S. S. Rao, R. S. Blumberg, J. R. Mascola, G. J. Nabel, Enhanced neonatal Fc receptor function improves protection against primate SHIV infection. *Nature* **514**, 642-645 (2014).
23. R. S. Rudicell, Y. D. Kwon, S. Y. Ko, A. Pegu, M. K. Louder, I. S. Georgiev, X. Wu, J. Zhu, J. C. Boyington, X. Chen, W. Shi, Z. Y. Yang, N. A. Doria-Rose, K. McKee, S. O'Dell, S. D. Schmidt, G. Y. Chuang, A. Druz, C. Soto, Y. Yang, B. Zhang, T. Zhou, J. P. Todd, K. E. Lloyd, J. Eudailey, K. E. Roberts, B. R. Donald, R. T. Bailer, J. Ledgerwood, N. C. S. Program, J. C. Mullikin, L. Shapiro, R. A. Koup, B. S. Graham, M. C. Nason, M. Connors, B. F. Haynes, S. S. Rao, M. Roederer, P. D. Kwong, J. R. Mascola, G. J. Nabel, Enhanced potency of a broadly neutralizing HIV-1 antibody *in vitro* improves protection against lentiviral infection *in vivo*. *J. Virol.* **88**, 12669-12682 (2014).
24. M. Caskey, F. Klein, J. C. Lorenzi, M. S. Seaman, A. P. West, Jr., N. Buckley, G. Kremer, L. Nogueira, M. Braunschweig, J. F. Scheid, J. A. Horwitz, I. Shimeliovich, S. Ben-Avraham, M. Witmer-Pack, M. Platten, C. Lehmann, L. A. Burke, T. Hawthorne, R. J. Gorelick, B. D. Walker, T. Keler, R. M. Gulick, G. Fatkenheuer, S. J. Schlesinger, M. C. Nussenzweig, Viraemia suppressed in HIV-1-infected humans by broadly neutralizing antibody 3BNC117. *Nature* **522**, 487-491 (2015).
25. R. Shankarappa, J. B. Margolick, S. J. Gange, A. G. Rodrigo, D. Upchurch, H. Farzadegan, P. Gupta, C. R. Rinaldo, G. H. Learn, X. He, X. L. Huang, J. I. Mullins, Consistent viral evolutionary changes associated with the progression of human immunodeficiency virus type 1 infection. *J. Virol.* **73**, 10489-10502 (1999).

26. M. Caskey, T. Schoofs, H. Gruell, A. Settler, T. Karagounis, E. F. Kreider, B. Murrell, N. Pfeifer, L. Nogueira, T. Y. Oliveira, G. H. Learn, Y. Z. Cohen, C. Lehmann, D. Gillor, I. Shimeliovich, C. Unson-O'Brien, D. Weiland, A. Robles, T. Kummerle, C. Wyen, R. Levin, M. Witmer-Pack, K. Eren, C. Ignacio, S. Kiss, A. P. West, Jr., H. Mouquet, B. S. Zingman, R. M. Gulick, T. Keler, P. J. Bjorkman, M. S. Seaman, B. H. Hahn, G. Fatkenheuer, S. J. Schlesinger, M. C. Nussenzweig, F. Klein, Antibody 10-1074 suppresses viremia in HIV-1-infected individuals. *Nat. Med.* **23**, 185-191 (2017).
27. J. N. Bhiman, R. M. Lynch, Broadly neutralizing antibodies as treatment: effects on virus and immune system. *Curr. HIV/AIDS Rep.* **14**, 54-62 (2017).
28. D. I. Rosenbloom, A. L. Hill, S. A. Rabi, R. F. Siliciano, M. A. Nowak, Antiretroviral dynamics determines HIV evolution and predicts therapy outcome. *Nat. Med.* **18**, 1378-1385 (2012).
29. Y. Bar-On, H. Gruell, T. Schoofs, J. A. Pai, L. Nogueira, A. L. Butler, K. Millard, C. Lehmann, I. Suarez, T. Y. Oliveira, T. Karagounis, Y. Z. Cohen, C. Wyen, S. Scholten, L. Handl, S. Belblidia, J. P. Dizon, J. J. Vehreschild, M. Witmer-Pack, I. Shimeliovich, K. Jain, K. Fiddike, K. E. Seaton, N. L. Yates, J. Horowitz, R. M. Gulick, N. Pfeifer, G. D. Tomaras, M. S. Seaman, G. Fatkenheuer, M. Caskey, F. Klein, M. C. Nussenzweig, Safety and antiviral activity of combination HIV-1 broadly neutralizing antibodies in viremic individuals. *Nat. Med.* **24**, 1701-1707 (2018).
30. P. Mendoza, H. Gruell, L. Nogueira, J. A. Pai, A. L. Butler, K. Millard, C. Lehmann, I. Suarez, T. Y. Oliveira, J. C. C. Lorenzi, Y. Z. Cohen, C. Wyen, T. Kummerle, T. Karagounis, C. L. Lu, L. Handl, C. Unson-O'Brien, R. Patel, C. Ruping, M. Schlotz, M. Witmer-Pack, I. Shimeliovich, G. Kremer, E. Thomas, K. E. Seaton, J. Horowitz, A. P. West, Jr., P. J. Bjorkman, G. D. Tomaras, R. M. Gulick, N. Pfeifer, G. Fatkenheuer, M. S. Seaman, F. Klein, M. Caskey, M. C. Nussenzweig, Combination therapy with anti-HIV-1 antibodies maintains viral suppression. *Nature* **561**, 479-484 (2018).
31. N. L. Haigwood, Antibodies pose a double threat to HIV. *Nature* **561**, 468-470 (2018).
32. E. N. Borducchi, J. Liu, J. P. Nkolola, A. M. Cadena, W. H. Yu, S. Fischinger, T. Broge, P. Abbink, N. B. Mercado, A. Chandrashekar, D. Jetton, L. Peter, K. McMahan, E. T. Moseley, E. Bekerman, J. Hesselgesser, W. Li, M. G. Lewis, G. Alter, R. Geleziunas, D. H. Barouch, Antibody and TLR7 agonist delay viral rebound in SHIV-infected monkeys. *Nature* **563**, 360-364 (2018).
33. M. N. Wykes, S. R. Lewin, Immune checkpoint blockade in infectious diseases. *Nat. Rev. Immunol.* **18**, 91-104 (2018).
34. G. Mutua, B. Farah, R. Langat, J. Indangasi, S. Ogola, B. Onsembe, J. T. Kopycinski, P. Hayes, N. J. Borthwick, A. Ashraf, L. Dally, B. Barin, A. Tillander, J. Gilmour, J. De Bont, A. Crook, D. Hannaman, J. H. Cox, O. Anzala, P. E. Fast, M. Reilly, K. Chinyenze, W. Jaoko, T. Hanke, Broad HIV-1 inhibition in vitro by vaccine-elicited CD8+ T cells in African adults. *Mol. Ther. Methods Clin. Dev.* **3**, 16061 (2016).
35. F. Garcia, N. Climent, A. C. Guardo, C. Gil, A. Leon, B. Autran, J. D. Lifson, J. Martinez-Picado, J. Dalmau, B. Clotet, J. M. Gatell, M. Plana, T. Gallart, D. M. O. S. Group, A dendritic cell-based vaccine elicits T cell responses associated with control of HIV-1 replication. *Sci. Transl. Med.* **5**, 166ra162 (2013).
36. H. Murakoshi, C. Zou, N. Kuse, T. Akahoshi, T. Chikata, H. Gatanaga, S. Oka, T. Hanke, M. Takiguchi, CD8(+) T cells specific for conserved, cross-reactive Gag epitopes with strong ability to suppress HIV-1 replication. *Retrovirology* **15**, 46 (2018).

37. E. Pan, F. Feng, P. Li, Q. Yang, X. Ma, C. Wu, J. Zhao, H. Yan, R. Chen, L. Chen, C. Sun, Immune protection of SIV challenge by PD-1 blockade during vaccination in rhesus monkeys. *Front. Immunol.* **9**, 2415 (2018).
38. B. Mothe, C. Brander, in *HIV Vaccines and Cure : The Path Towards Finding an Effective Cure and Vaccine*, L. Zhang, S. R. Lewin, Eds. (Springer Singapore, Singapore, 2018), 10.1007/978-981-13-0484-2_2, pp. 31-51.
39. T. Schoofs, F. Klein, M. Braunschweig, E. F. Kreider, A. Feldmann, L. Nogueira, T. Oliveira, J. C. Lorenzi, E. H. Parrish, G. H. Learn, HIV-1 therapy with monoclonal antibody 3BNC117 elicits host immune responses against HIV-1. *Science* **352**, 997-1001 (2016).
40. G. Doitsh, N. L. Galloway, X. Geng, Z. Yang, K. M. Monroe, O. Zepeda, P. W. Hunt, H. Hatano, S. Sowinski, I. Muñoz-Arias, Cell death by pyroptosis drives CD4 T-cell depletion in HIV-1 infection. *Nature* **505**, 509 (2014).
41. S. Wang, P. Hottz, M. Schechter, L. Rong, Modeling the slow CD4+ T cell decline in HIV-infected individuals. *PLoS Comput. Biol.* **11**, e1004665 (2015).
42. M. P. Davenport, R. M. Ribeiro, A. S. Perelson, Kinetics of virus-specific CD8+ T cells and the control of human immunodeficiency virus infection. *J. Virol.* **78**, 10096-10103 (2004).
43. L. Zhang, P. J. Dailey, T. He, A. Gettie, S. Bonhoeffer, A. S. Perelson, D. D. Ho, Rapid clearance of simian immunodeficiency virus particles from plasma of rhesus macaques. *J. Virol.* **73**, 855-860 (1999).
44. M. J. Bevan, Helping the CD8+ T-cell response. *Nat. Rev. Immunol.* **4**, 595 (2004).
45. P. L. F. Johnson, B. F. Kochin, M. S. McAfee, I. M. Stromnes, R. R. Regoes, R. Ahmed, J. N. Blattman, R. Antia, Vaccination alters the balance between protective immunity, exhaustion, escape, and death in chronic infections. *J. Virol.* **85**, 5565-5570 (2011).
46. T. R. Mempel, S. E. Henrickson, U. H. Von Andrian, T-cell priming by dendritic cells in lymph nodes occurs in three distinct phases. *Nature* **427**, 154 (2004).
47. E. J. Wherry, M. Kurachi, Molecular and cellular insights into T cell exhaustion. *Nature Reviews Immunology* **15**, 486 (2015).
48. R. Mostowy, R. D. Kouyos, D. Fouchet, S. Bonhoeffer, The role of recombination for the coevolutionary dynamics of HIV and the immune response. *PLoS One* **6**, e16052 (2011).
49. C. L. Althaus, R. J. De Boer, Dynamics of immune escape during HIV/SIV infection. *PLoS Comput. Biol.* **4**, e1000103 (2008).